Journal of Physics: Conference Series **2462** (2023) 012026 doi:10.1088/1742-6596/2462/1/012026

# Intense Lyman-alpha light source for ultra-slow muon generation

**Y Oishi[1,3,4], T Adachi[5], N Saito[4], Y Ikedo[1,3], K Ishida[5], S Kanda[1,3], T Umezawa[6], S Kamioka[2], N Teshima[1,3], J Nakamura[1,3], S Nakamura[6], Y Miyake[1,3], M Iwasaki[5], S Wada[4], K Shimomura[1,3]**

[1] Muon Science Laboratory, Institute of Materials Structure Science, High Energy Accelerator Research Organization (KEK), 1-1 Oho, Tsukuba, Ibaraki 305-0801, Japan

[2] Muon-Neutron Group, Institute of Particle and Nuclear Studies, High Energy Accelerator Research Organization (KEK), 1-1 Oho, Tsukuba, Ibaraki 305-0801, Japan

[3] Muon Science Section, Materials and Life Science Division, J-PARC Center, 2-4 Shirane Shirakata, Tokai, Naka, Ibaraki 319-1195, Japan

[4] Center for Advanced Photonics, RIKEN, 2-1 Hirosawa, Wako, Saitama 351-0198, Japan

[5] Nishina Center for Accelerator-based Science, RIKEN, 2-1 Hirosawa, Wako, Saitama 351-0198, Japan

[6] College of Engineering, Ibaraki University, 4-12-1 Nakanarusawa, Hitachi, Ibaraki 316-8511, Japan
E-mail : bigstone@post.kek.jp

**Abstract**. A small-momentum-width muon beam, so-called ultra-slow muon beam, can be generated by laser ionization of muonium. To realize efficient ultra-slow muon generation, the Lyman-alpha and below 360 nm coherent light are required to resonantly excite the muonium from the ground state to 2*p* and sequentially ionizes excited muonium to the unbound state. At the J-PARC MLF Ultra-Slow Muon beamline, we have successfully generated Lyman-alpha coherent light exceeding 10 μJ using an all-solid-state laser and high-efficiency vacuum ultraviolet light generation technologies. In this paper, we will describe the intense Lyman-alpha light source.

## 1. Introduction
Muons are spontaneously 100% spin-polarized at the time of generation, making them an innovative magnetic probe particle that can directly measure the local magnetic field distribution from the interface/surface to the interior of a material on an atomic scale when injected into the material [1]. However, it has been difficult to measure the physical properties of nano-scale interfaces and thin films with high spatial resolution because the energy dispersion of slow muon beam results in a wide stopping

depth. The development of low-energy muon or ultra-slow muon beams to overcome such problems is still underway, which is expected to lead to new developments in material science. Conventional low-energy muon has been produced by a low-temperature solid-state deceleration method [2, 3], but in principle there are problems with energy dispersion, time resolution, and production efficiency. On the other hand, the laser ionization method, which overcomes the above problems, uses 4-MeV muons which stop inside a muonium production target (2000 K heated tungsten foil), and ~0.2 eV muonium (hydrogen-like bound state of a positive muon and an electron) that thermally evaporates into the vacuum is produced. The muonium is irradiated by resonant excitation and ionization laser beams to efficiently dissociate the electrons. The excitation laser light requires muonium Lyman-α (Ly-α) resonant vacuum ultraviolet coherent light (122.09 nm), which corresponds to the 1*s*-2*p* level difference of muonium. A Ly-α light source with an output power of <1 μJ based on a flashlamp-pumped Nd:YAG laser and a Ti:sapphire amplifier has been used in the past, but it has problem in long term stability [4]. In this paper, we describe an intense Ly-α coherent light source to be used in the high-intensity ultra-slow muon production experiment at the Japan Proton Accelerator Research Complex (J-PARC).

## 2. Generation of pulsed Lyman-alpha

The wavelength of the Ly-α resonance line of muonium (122.09 nm) is in the vacuum ultraviolet region, and since there are no solid-state nonlinear optical crystals as well as laser media that can directly emit this wavelength, harmonic generation in gases, four-wave-mixing in Kr or Xe gas or in mercury vapor, etc. have been used [5-8]. In particular, it is known that the generation efficiency of vacuum ultraviolet light by two-photon resonant four-wave-mixing (FWM) using the energy levels between the ground levels $4s^6$ and $4p^5$-$5p[1/2,0]$ of Kr is generally two orders of magnitude higher than that without resonant excitation. Therefore, we have decided to construct a light source using two-photon resonant FWM in Kr gas for the generation of intense Ly-α light due to its efficiency and simplicity of the device.

Two-photon resonant FWM is a third-order nonlinear optical effect that generates Ly-α light $\omega_{\mathrm{Ly}}$ by using two-photon resonant excitation light $\omega_1$ and mixed light $\omega_2$. The relation of frequencies is satisfied $2\omega_1$-$\omega_2$=$\omega_{\mathrm{Ly}}$ [8]. The difference between the $4s^6$ and $4p^5$-$5p[1/2,0]$ energy levels of Kr is 11.6675 eV, and the corresponding wavelength of $\omega_1$ is 212.556 nm. The Ly-α wavelength of muonium is determined to be 122.089 nm based on the converted masses of protons and muons, and $\omega_2$ is determined to have a wavelength of 820.649 nm from the relation $2\omega_1$-$\omega_2$=$\omega_{\mathrm{Ly}}$. The energy diagram of two-photon resonant FWM in Kr gas for Ly-α generation is shown in figure 1[9]. In other words, it is necessary to build a laser that generates intense $\omega_1$(212.556 nm) and $\omega_2$(820.649 nm).

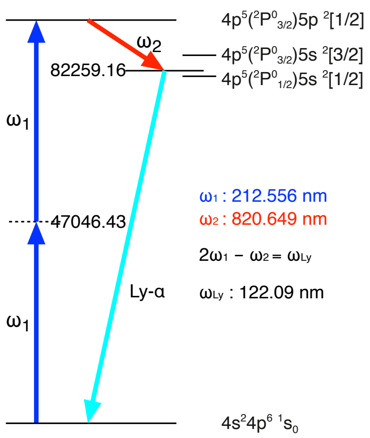


Figure 1. Energy diagram of two-photon resonance FWM in Kr gas to generate muonium Ly-α photons.

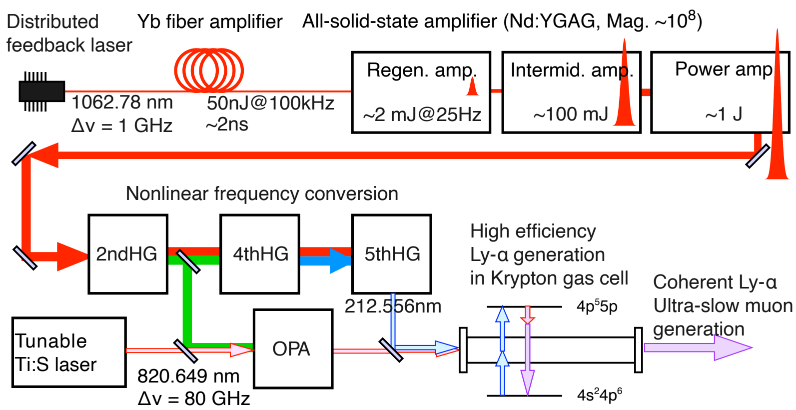


Figure 2. The schematic of intense Ly-α light source. The system consists of wavelength stable laser diode (LD), fiber amplifier, all-solid-state laser amplifiers with special gain medium, nonlinear wavelength conversions and high-efficient Ly-α generation.

## 3. All-solid-state laser for Lyman-α generation

In order to achieve saturated ionization condition of muonium, 100 $\mu$J pulse energy is required with Ly-α light, which is two orders of magnitude higher than the muonium Ly-α light source at RIKEN muon facility in Rutherford Appleton Laboratory (RIKEN-RAL). Considering the FWM efficiency in RIKEN-RAL ($10^{-5}$) and Ref. 5 ($10^{-4}$), it is necessary to generate at least 100 mJ each for $\omega_1$ and $\omega_2$. Since the wavelength of $\omega_1$ is 1062.78 nm when multiplied by 5, and the Nd-based as pumped solid-state laser technology is applicable, we decided to generate $\omega_1$ by nonlinear frequency conversion using a 1 J-class 1062.78 nm pulse. Figure 2 shows an overview of the light source. A precisely wavelength locked laser light is amplified by a fiber amplifier and an all-solid-state amplifier, and $\omega_1$ is output by generating the fifth harmonic using a multi-stage nonlinear frequency conversion. $\omega_2$ is obtained by parametric amplification using a part of the output of the first stage nonlinear frequency conversion as the pump light. The system is designed to generate $\omega_1$ and $\omega_2$ from the same pulse to eliminate the jitter between the pulses and to achieve high stability in the subsequent FWM in the Kr gas. The elements in all solid-state laser part are described below.

### *3.1. Oscillator and fiber pre-amplifier*

To achieve highly efficient two-photon resonant excitation of Kr gas, a fiber-coupled mode-hop-free distributed feedback semiconductor laser with an oscillation wavelength of 1062.78 nm and a spectral linewidth of 1 GHz was introduced at the upstream of the system. The wavelength of the laser light obtained from the distributed feedback laser was stabilized by adjusting the chip temperature and injection current with a minimum resolution of less than 1 pm on a wavelength meter (HighFinessWS-6). The pulse energy was increased by using multiple stages Yb fiber amplifiers. The pulse repetition rate and pulse width were set to 100 kHz and 2.6 ns, respectively, to suppress nonlinear effects inside the fiber and to avoid optical damage. The output pulse energy is 50 nJ/pulse, and amplification to higher energy levels is performed by an all-solid-state amplifier output in free space. The operation of the system after the regenerative amplifier described below is synchronized with the proton accelerator operation at 25 Hz.

### *3.2. Regenerative amplifier*

A regenerative amplifier was introduced in the first stage of the all-solid-state amplifier for high gain, beam quality, and pointing stability. For a highly efficient amplification, the gain medium of all-solid-state amplifier requires a laser crystal with the maximum gain at 1062.78 nm. Since the generally used Nd:YAG laser medium does not provide sufficient gain at 1062.78 nm, $Nd:Y_3Sc_2Al_3O_{12}$ (Nd:YSAG) and $Nd:Y_3Ga_2Al_3O_{12}$ (Nd:YGAG) which have been reported in spectroscopic evaluations were studied as amplifiers gain medium[10,11]. The fluorescence spectra of the 1at.%Nd-doped YSAG, YGAG, and YAG crystals are shown in Figure 3. The fluorescence cross sections at 1062.78 nm were $0.8 \times 10^{-19}$ $cm^2$ and $1.1 \times 10^{-19}$ $cm^2$ for YSAG and YGAG, respectively, compared to $0.3 \times 10^{-19}$ $cm^2$ for YAG. The regenerative amplifier was designed to be a stable resonator with a resonator length (2.1 m) sufficient to confine the 2.6 ns pulse output from the fiber amplifier. From point of view of fluorescence cross section, the Nd:YGAG crystals were applied as amplifier gain medium ($4 \times 4 \times 10$ $mm^3$) and end-pumped by two fiber-coupled LDs (808 nm, 25 Hz quasi-continuous-wave). The input 50 nJ seed pulse was successfully amplified up to 2.4 mJ with 25 mJ pump

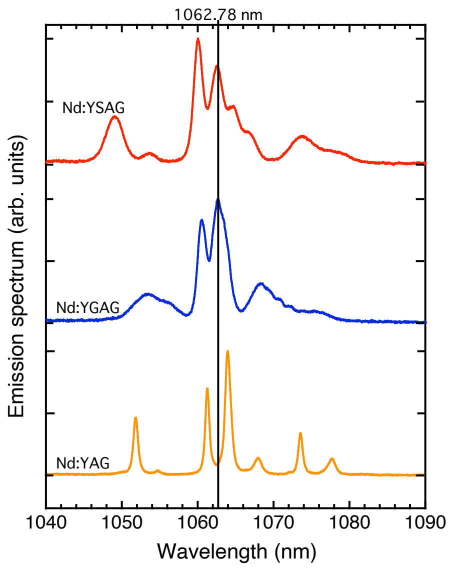


Figure 3. Emission spectrum of Nd:YAG, Nd:YGAG and Nd:YSAG.

energy. The center wavelength of the amplified pulse was 1062.78 nm, the same as the incident seed pulse.

### *3.3. Intermediate amplifier*

Approximately 2 mJ pulse from the regenerative amplifier was amplified to a level of 100 mJ using intermediate amplifier. The pumping chamber consists of a gain medium with a diameter of 4 mm and a length of 80 mm, which is pumped from three sides by six stacked LD bars (peak power 1 kW at 25 Hz). Nd:YGAG is suitable for the gain medium of 1062.78 nm, but it was difficult to obtain transparent Nd:YGAG single crystals of this size because of the difficulty in controlling the gallium concentration during the crystal growth. To solve this problem, we fabricated Nd:YGAG rods using a novel ceramic technology and realized amplification while maintaining high beam quality. The pulse from the regenerative amplifier is passed through a polarizingref beam splitter (PBS) and injected into the gain medium of the first amplification chamber. The amplified pulse is reinjected into the same gain medium by a normal-incidence mirror and amplified again. When the pulse is folded back by the mirror, the reinjected pulse polarization is 90° rotated by the waveplate, so that the amplified pulse is totally reflected by the PBS and sent to the second amplification chamber. The reflected amplified pulse is passed through another gain medium of the second amplification chamber. A maximum output of 106 mJ was obtained for a total pump energy of 2.5 J by passing through the gain region a total of three times. The output spatial beam profile was nearly circular with a diameter of 1.8 mm and $M^2$=1.3, and the pulse width was about 2.2 ns. The required pulse energy of the light source is in the 1 J-level, but due to quality issues with the large aperture Nd:YGAG laser ceramic for the final stage amplifier, the output from the intermediate amplifier was used to perform this subsequent wavelength conversion.

### *3.4. 212.556 nm pulse generation*

The 100 mJ pulse with wavelength of 1062.78 nm from the intermediate amplifier was applied to generate 212.556 nm pulse by wavelength conversion using multiple nonlinear crystals. After the beam diameter of the fundamental pulse was expanded and collimated to 4.5 mm by a lens pair, the second harmonic pulse (531.39 nm) was generated with 60% of conversion efficiency using a $LiB_3O_5$ (LBO) crystal ($15 \times 15 \times 20$ mm$^3$, $\theta = 90°$, $\phi = 0°$) [12] whose temperature was controlled to achieve noncritical phase matching conditions. Half of the second harmonic pulse was used for nonlinear frequency conversion for $\omega_1$ generation, and the other half was used as pump pulse for $\omega_2$ generation. 30 mJ second harmonic pulse was converted to the fourth harmonic pulse using $CsLiB_6O_{10}$ (CLBO) crystal (15×15×15 mm$^3$, $\theta$ = 62.2°, $\phi$ = 45°). Subsequently, the converted 8.7 mJ fourth harmonic pulse and, 35 mJ of 1062.78 nm pulse that was not converted to the second harmonic by the LBO crystal were injected into another CLBO crystal (15 × 15 × 15 mm$^3$, $\theta$ = 68.5°, $\phi$ = 45°) to generate the fifth harmonic pulse. Finally, 3.2 mJ fifth harmonic pulse was obtained. These CLBO crystals used for the fourth and fifth harmonic generation were sealed in a dry cell with a strictly dehumidified atmosphere and kept at a temperature of 150±0.1°C. The obtained $\omega_1$ pulse energy has been stable for more than seven years without any significant optical degradation of the nonlinear crystals.

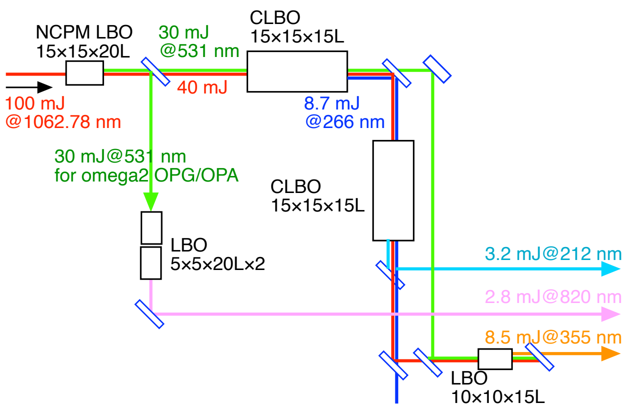

Figure 4. The schematic of nonlinear wavelength conversions. The optical pass length of $\omega_1$ and $\omega_2$ to achieve timing jitter free for Ly-α generation

### *3.5. 820.65 nm pulse generation*

In order to achieve resonant excitation of muonium, it is necessary to optimize the wavelength of $\omega_{Ly}$. A tunable Ti:sapphire laser was introduced as a seeder of $\omega_2$ to control the central wavelength. The output wavelength from the seeder was tuned by the yield of ultra-slow muons. For parametric amplification, pump pulse (10 mJ, 25 Hz, $\Delta\tau = 2.2$ ns) was injected into two LBO crystals ($5 \times 5 \times 20$ mm$^3$, $\theta = 90°$, $\phi = 0°$) placed in series with a beam diameter of approximately 1.1 mm. The crystals temperature was adjusted to 119.6±0.1°C to keep the output central wavelength of the parametric generation near 820.65 nm. The crystal faces were coated with anti-reflection coatings for the pump, signal, and idler wavelengths, and only the 820 nm amplified pulse was extracted by a dichroic mirror. When the timing and mode of seed pulse (10 μJ, 250 Hz, $\lambda \simeq 820$ nm, $\Delta\nu \simeq 80$ GHz) was matched to pump pulse (10 mJ, 25 Hz), a maximum pulse energy of 2.8 mJ was obtained.

### *3.6. 355 nm pulse generation*
For the ultra-slow muon generation process, not only the Ly-α pulse but also below 360 nm pulse is required. The all-solid-state light source can provide timing jitter free 355 nm pulses (8 mJ/pulse) using the residual 1062.78 nm and 531.39 nm pulses in the wavelength conversion process. The schematic of nonlinear wavelength conversions is shown in Figure 4.

## **4. Lyman-alpha light generation**
The generated pulses from the all-solid-state laser were transported to the radiation-shielded area to generate Ly-α pulse. The schematic view of the Ly-α generator and the ultra-slow muon generation is shown in Figure 5. The $\omega_1$ and $\omega_2$ pulses were spatiotemporally superposed and focused into the center of 1 m long gas cell with loose focusing configuration. For temporal overlapping, the optical path lengths of $\omega_1$ and $\omega_2$ were adjusted with an accuracy of <5 mm. To increase the generated Ly-α pulse intensity, Ar gas was mixed to Kr gas to satisfy the phase matching condition. Under our conditions, the highest conversion efficiency was obtained at Kr:Ar = 1:5.5, and the optimum mixture gas pressure was about 2200 Pa. The Ly-α pulse was generated coaxially with the incident $\omega_1$ and $\omega_2$ pulses. To separate from incident pulses, a 6° wedged window (LiF, t=8 mm, T≃40%@122 nm) was used as an output window. The spatially separated Ly-α pulse in ultrahigh vacuum was steered by flat and cylindrical mirrors to the muonium ionization region. These mirrors were coated with enhanced aluminum ($Al+MgF_2$, R≃80%@122 nm). The shaped beam was measured by inserting a dielectric mirror in the optical path and was reflected to a sodium salicylate fluorescent plate which was placed at a position equivalent to the ionization region. The pulse energy of the Ly-α was measured by inserting a sensitivity calibrated photodiode (OptoDiodeInc., SXUV-300).
The actual $\omega_1$ and $\omega_2$ pulse energies injected into the gas cell were 1.6 mJ and 2.1 mJ, respectively, due to losses in mirrors, focusing lens and beam combiner. The measured maximum pulse energy of Ly-α reached 5 μJ which include losses of the window at the exit of the gas cell and two steering mirrors. The conversion efficiency from $\omega_1$ to Ly-α at immediately after the exit window of the gas cell was almost $5\times10^{-3}$ [13]. This high conversion efficiency was achieved because the beam obtained from the all-solid-state laser is of high quality, which makes it easy to control the propagation with focusing, suppresses ionization of Kr gas due to hot spots, etc., and at the same time, short pulses and low jitter are achieved.

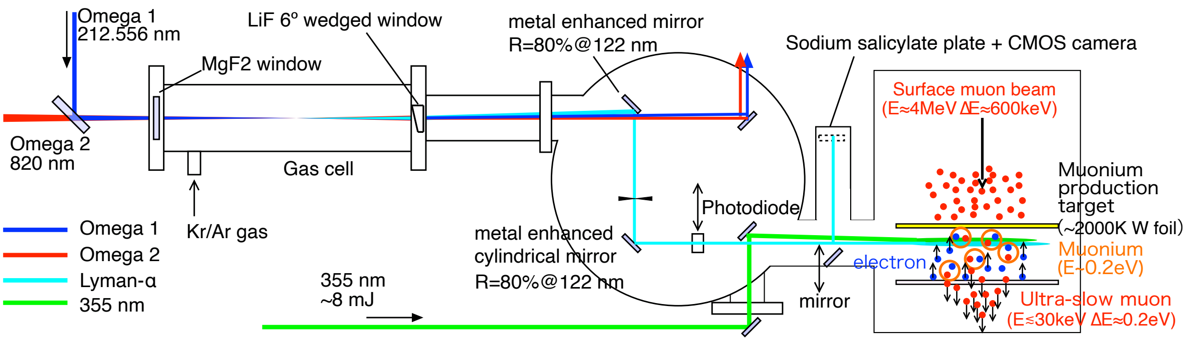


Figure 5. The experimental setup of Ly-α generation and ultra-slow muon generation. The beam overlap and shape is confirmed by observation of the sodium salicylate fluorescent plate image.

## 5. Lyman-alpha beam steering and ultra-slow muon generation

To increase the yield of ultra-slow muons, the Ly-α and the 355 nm beams were shaped by a cylindrical mirror and lens, respectively. The measured Ly-α beam profile (8.7 mm in vertical and 2.0 mm in horizontal direction) is shown in Figure 6. The Ly-α and the 355 nm beams were spatially superposed with an angle of approximately 30 mrad, and were propagated parallel to a muonium production target (70 mm wide and 40 mm height). The generated ultra-slow muons by photoionization were electrostatically accelerated to 30 keV, and the generation yield was measured by a micro channel plate detector. To determine the resonance wavelength of muonium, the center wavelength of $\omega_2$ was swept from 819.4 nm to 822.0 nm at intervals of about 0.2 nm. When the wavelength of $\omega_2$ was 820.6 nm, the maximum yield of ultra-slow muon was obtained. The wavelength of muonium Ly-α was determined to be 122.088 nm. Applying the pulses irradiation conditions to the ionization rate equation, it is calculated that about 20% of the muonium in the optical pass volume is converted to ultra-slow muon. The apparatus and experiment of ultra-slow muon generation is described in Ref. [14].

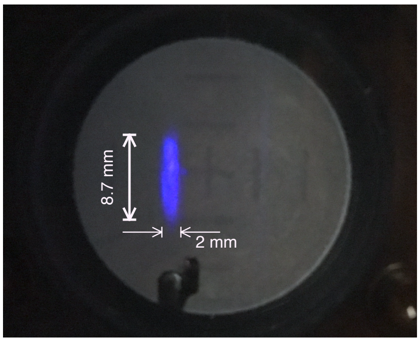


Figure 6. The Ly-α beam profile at muonium ionization region.

## 6. Summary

In this paper, we introduce an intense Lyman-α coherent light source for the generation of ultra-slow muons. The light source consists of an all-solid-state laser part and the Ly-α generation using two-photon resonant four-wave mixing in Kr gas. In the all-solid-state laser section, Nd:YGAG ceramic was developed as a medium to efficiently amplify the 1062.78nm pulse, and was the first amplifier crystal to be put to practical use, achieving an output power exceeding 100 mJ. In the wavelength conversion section, timing jitter free 212.556 nm and 820.65 nm pulses were generated for stable two-photon resonant four-wave mixing. In the feature of a long interaction length by a long-focus configuration, the generation of Ly-α achieved a high conversion efficiency of $5\times10^{-3}$ and a pulse energy level of 10 μJ. The successful stable generation of ultra-slow muons using this light source and the muon beam at J-PARC has raised expectations for further developmental research in fundamental physics and condensed matter experiments in the future.

## References

[1] Miyake Y, et al. Rad. Phys. Chem., 60 (2001) 521-524.
[2] Morenzoni E, et al, J. Phys.: Cond. Matt. 16, S4583 (2004)
[3] Prokscha T, et al, NIM A 595, 317 (2008)
[4] Bakule P, et al. Nucl. Instrum. Meth. Phys. Res. B, 266 (2008) 335-346.
[5] Marangos J P, J. Opt. Soc. Am. B, 7 (1990) 1254-1259.
[6] Miyazaki K, et al. Appl. Opt., 2 (1989) 699-702.
[7] Scheid M, et al. Opt. Lett., 32 (2007) 955-957.
[8] Reintjes J F, Academic Press, London (1984).
[9] Mohr P, et al. J. Phys. Chem. Ref. Data, 45 (2016) 043102-1-74.
[10] Sato Y, et al. Opt. Mater., 29 (2007) 1277-1282.
[11] Walsh B M, et al. J. Opt. Soc. Am. B, 15 (1998) 2794-2801.
[12] Mori Y, et al. Appl. Phys. Lett., 67 (1995) 1818-1820.
[13] Saito N, et al. Opt. Exp., 24 (2016) 7566-7574.
[14] Kanda S et al., J. Phys.: Conf. Ser. this issue.